Heliyon 10 (2024) e38379

Contents lists available at ScienceDirect

Heliyon

journal homepage: www.cell.com/heliyon

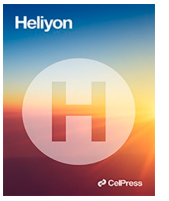

Research article

Daucosterol alleviates heart failure with preserved ejection fraction through activating PPARα pathway

Jie Zhou [a,1], Bei Wang [b,1], Mengyao Wang [a], Yang Zha [a], Shengyuan Lu [a], Feng Zhang [a], Ying Peng [a], Yajun Duan [c], Dingrong Zhong [b,**], Shuang Zhang [a,*]

[a] Key Laboratory of Metabolism and Regulation for Major Diseases of Anhui Higher Education Institutes, College of Food and Biological Engineering, Hefei University of Technology, Hefei, China
[b] Department of Pathology, China-Japan Friendship Hospital, Beijing, China
[c] Department of Cardiology, The First Affiliated Hospital of University of Science and Technology of China, Hefei, China

ARTICLE INFO

Keywords:
Daucosterol
HFpEF
Inflammation
PPARα
NF-κB

ABSTRACT

Heart failure with preserved ejection fraction (HFpEF) has been increasing in the population in recent years and is mainly characterized by preserved left ventricle ejection fraction (LVEF), diastolic dysfunction and systemic inflammation. Daucosterol (DAU), a glycoside of β-sitosterol, has good anti-inflammatory and antioxidative properties; however, its effects and mechanisms in HFpEF have not been investigated. To detect whether DAU could alleviate HFpEF, C57BL/6J male mice were fed with N-nitro-l-arginine methyl ester (L-NAME) in drinking water and high fat diet (HFD) and treated with DAU by gavage (i.g.) for 10 weeks. The results showed that DAU treatment significantly alleviated HFpEF in mice. Mechanistically, by controlling PPARα and preventing NF-κB phosphorylation, DAU reduced oxidative stress and the inflammatory response. In conclusion, our study provides a new clue for natural product DAU in alleviating HFpEF.

1. Introduction

Heart failure is the major cause of morbidity and mortality globally. According to epidemiology, almost 50 % of patients have heart failure with preserved ejection fraction (HFpEF), and the prevalence of this condition has been rising recently [1]. HFpEF is a heterogeneous clinical syndrome with unmet diagnostic and therapeutic needs [2]. The fundamental cause of its pathophysiology is malfunction of the ventricles during diastole, either at rest or under pressure. Although HFpEF has a normal ejection fraction at rest, it does not improve when the pressure load increases, and other parameters of systolic function are abnormal [3]. HFpEF is also regarded as a systemic syndrome [4], there are currently few effective therapies to address this widespread issue and a lack of understanding of the underlying processes. Recently, it has been reported that myocardial cell stiffness, cellular hypertrophy and myocardial fibrosis caused by myocardial inflammation, oxidative stress and coronary artery endothelial dysfunction are the main mechanisms of HFpEF [5,6]. Firstly, distinct cardiac cells can become inflammatory and undergo subcellular changes because of increased levels of pro-inflammatory cytokines and metabolic substrates. Subcellular changes then stimulate maladaptive myocardial remodeling, and long-term low-grade inflammation gradually modifies the heart's metabolic functions, culminating in a metabolic cardiomyopathy

* Corresponding author.
** Corresponding author.
E-mail addresses: 748803069@qq.com (D. Zhong), zhangshuang@hfut.edu.cn (S. Zhang).
[1] These authors contributed equally to this work.

https://doi.org/10.1016/j.heliyon.2024.e38379
Received 22 April 2024; Received in revised form 23 September 2024; Accepted 23 September 2024
Available online 24 September 2024

phenotype and ultimately HFpEF [7]. Therefore, there is a greater potential to treat HFpEF from systemic inflammation, myocardial fibrosis, and oxidative stress.

Daucosterol (DAU) is a glycoside of natural β-sitosterol, mainly synthesized by plants such as carrot, herbaceous peony, Dan-Shen root, *etc*. DAU have been shown to have strong anti-inflammatory and antioxidant properties in earlier research. After extracting DAU from *Sanchezia speciosa*, Bui et al. used the 2,2-diphenyl-1-picrylhydrazyl (DPPH) technique to assess DAU's antioxidant ability [8]. In addition, DAU can inhibit colitis-induced ROS and inflammatory cytokines such as tumor necrosis factor-alpha (TNF-α), interleukin-1 beta (IL-1β), interleukin-6 (IL-6), interferon-γ (IFN-γ) increasement while regulating immune T-cells numbers and reducing macrophage infiltration [9]. Our previous study also found that DAU could reduce alcohol-induced liver inflammation through the p38/NF-κB/NLRP3 pathway [10].

As of right now, DAU serves a variety of purposes and exhibits good anti-inflammatory and antioxidant properties, some of which are equivalent to those of currently used clinical drugs. However, it is uncertain whether DAU can be useful in alleviating HFpEF. Here, we investigated DAU's function in HFpEF and identified the underlying chemical mechanism. In summary, our findings point to DAU as a viable natural product for the treatment of HFpEF.

2. Materials and methods

2.1. Materials

Daucosterol (DAU, Cat# CSN10899) was purchased from CSN pharm (Chicago, IL, USA). High fat diet (HFD) (Cat# MD12033) was purchased from Medicience (Jiangsu, China). 3-(4,5-Dimethylthiazol-2-yl)-2,5-diphenyltetrazolium bromide (MTT) (Cat# M2003) was purchased from Sigma-Aldrich (Louis, MI, USA). Picrosirius Red staining kit (Cat# G1742) was purchased from Solarbio (Beijing, China). TUNEL Apoptosis Detection Kit (Cat# A113-01/02/03) was purchased from Vazyme Biotech Co., Ltd (Nanjing, China).

Rabbit anti-NF-κB (Cat# AF5006), p-NF-κB (Cat# AF2006), IL-6 (Cat# DF6087), Nrf2(Cat# AF0639), PGC1α (Cat# AF5395) antibodies were purchased from Affinity Biosciences, Inc. (Cincinnati, USA). Rabbit anti-PPARα (Cat# A6697), SOD2 (Cat# A1340), SOD1 (Cat# A0274), NLRP3 (Cat# A5652), TNFα (Cat# A0277) and IL-1β (Cat# A16288) antibodies were obtained from Abclonal (Wuhan, China). Rabbit anti-β-actin (Cat# 20536-1-AP) was obtained from Proteintech Group (Chicago, IL, USA).

2.2. In vivo studies

C57BL/6J male mice (7–8 weeks old, ~25 g body weight) were purchased from GemPharmatech Co., Ltd. (Nanjing, China). This research program has been officially approved by the Biological and Medical Ethics Committee of Hefei University of Technology, with approval number HFUT20220317001. All the experiments were not only conducted in the SPF animal experimental center of Hefei University of Technology, but all mice were kept in a light/dark cycle of 12 h at 22–24 °C and were given unlimited access to food and water.

The model of HFpEF was induced by HFD + L-NAME, a ' two-hit model '. The mice were fed with a HFD to induce obesity and impaired glucose tolerance, and the nitric oxide synthase inhibitor L-NAME was used to induce hypertension. The mice showed various typical characteristics of HFpEF, such as decreased diastolic function, decreased exercise capacity, pulmonary congestion and increased inflammatory factors in cardiac blood. In this model, the LVEF of mice remained normal [11].

Twenty 8-week-old C57BL/6J mice were randomly divided into four groups: normal control group (Control), dosed control group (DAU), HFpEF model group (HFpEF) and HFpEF model dosed group (HFpEF + DAU); HFpEF model was constructed by feeding HFD and water containing L-NAME (0.5 g/L) The dose of DAU (dissolved in corn oil) was 10 mg/kg in the normal group (each group of 5) and 10 mg/kg in the control group (each group of 5), and the dose of DAU was 10 mg/kg in the HFpEF model group (each group of 5) and 10 mg/kg in the HFpEF model + DAU group (each group of 5) for 5 weeks by gavage. The HFpEF model group and HFpEF model + DAU group were still fed HFD and water containing L-NAME during the gavage period.

2.3. Routine echocardiography and Doppler imaging

Transthoracic echocardiography was performed in mice using the Visual Sonics Vevo 2100 system equipped with an MS400 probe. The chest area of the mouse was prepared the day before the ultrasound to fully expose the heart position. Anesthesia was induced by 5 % isoflurane, and we confirmed its anesthetic status by observing the response of mice to hind paw stimulation. During the acquisition of echocardiography, we reduced the concentration of isoflurane to 1.0–1.5 % and adjusted its concentration to ensure that the heart rate of the mice was maintained in the range of 415–460 beats/min, while ensuring that the body temperature of the mice remained constant.

The orientation of the probe was changed, the left ventricle's long-axis view near the sternum was captured, and the short-axis M-scan at the ventricle's level was recorded to acquire the left ventricular ejection fraction and other systolic function indices. Measurements were made using tissue Doppler imaging at the mitral valve level and pulse wave to assess diastolic function. Heart rate, left ventricular end-diastolic and end-systolic diameter, left ventricular end-diastolic posterior wall, end-diastolic interventricular septum thickness, fractional shortening of the left ventricular, left ventricular ejection fraction, mitral diastolic peak blood flow velocity, isovolumic relaxation time, and myocardial tissue Doppler peak velocity during mitral annulus diastolic and early filling deceleration were among the many parameters we collected. After the operation, all mice recovered smoothly from anesthesia without any adverse reactions.

2.4. Blood pressure record

A tail cuff method and an animal noninvasive blood pressure monitor (BP98AWU, Tokyo, Japan) were used to assess blood pressure in conscious mice. Mice were placed in a mouse immobilizer and recorded under stable conditions until three stable continuous measurements were obtained.

2.5. Histochemical analysis

Mouse heart tissues were fixed in paraformaldehyde and embedded in paraffin. Sections were prepared and subjected to H&E staining, Sirius red staining and Masson staining[12,13]. Frozen heart tissues were sectioned to 7 μm for DHE staining [14].

2.6. Cell culture

Human cardiomyocytes AC16 cells (Cat # CL-0790) were provided by ATCC (Rockville, USA) and cultured in DMEM medium supplemented with 10 % fetal bovine serum and 50 mg/mL penicillin/streptomycin in a 5 % CO_2 incubator. AC16 cells were grouped and treated as follows: ①Control group (Ctrl): DMSO was added as a control; ②Control + inhibitor group (CP): 0.24 μmol/L of PPARα inhibitor was added to treat the cells for 24 h; ③Control drug group + inhibitor group (CPD): 1 μmol/L of DAU and 0.24 μmol/L of PPARα inhibitor were added to treat the cells for 24 h; ④Model group (LPS): 0.1 μmol/ml of lipopolysaccharide (LPS) was added to treat the cells for 24 h; ⑤Model + drug group (LD): 0.1 μmol/ml of LPS was added to treat the cells for 24 h and 0.1 μmol/ml of LPS and 0.24 μmol/L of PPARα inhibitor treated cells for 24 h; ⑥Model drug group + inhibition group (LDP): 0.1 μmol/ml of LPS, 1 μmol/L of carotene and 0.24 μmol/L of PPARα inhibitor treated cells for 24 h.

2.7. Cell viability assay

Cell viability was determined using the tetramethylazole salt colorimetric method described above [15]. After the indicated treatments, MTT solution (5 mg/mL/well) was added to the cells. Then 200 μl/well of dimethyl sulfoxide was added and shaken at low speed for 15 min, and the absorbance values were detected at a wavelength of 490 nm.

Table 1
Primer sequence used for RT-qPCR. M: mouse primers; H: human primers.

Gene	Forward primer	Reverse primer
Nrf2 (M)	TCACACGAGATGAGCTTAGGGCAA	TACAGTTCTGGGCGGCGACTTTA
PGC1α (M)	GATGACCCTCCTCACACCAA	AGTTGTGGGAGGAGTTAGGC
PPARα (M)	ACCTTGTGTATGGCCGAGAA	AAGGAGGACAGCATCGTGAA
SOD2 (M)	TCAATGGTGGGGGACATATT	GAACCTTGGACTCCCACAGA
SOD1 (M)	CCAGTGCAGGACCTCATTTT	TCATGGACCACCATTGTACG
NLRP3 (M)	CTCGCATTGGTTCTGAGCTC	AGTAAGGCCGGAATTCACCA
TNF-α (M)	ACTGAACTTCGGGGTGATCGGT	TGGTTTGCTACGACGTGGGCTA
IL-1β (M)	AGTTGCCTTCTTGGGACTGA	TCCACGATTTCCCAGAGAAC'
IL-6 (M)	AGACTTCCATCCAGTTGCCT	CATTTCCACGATTTCCCAGAGA
NF-κB (M)	CTGGCTACCACTGGAACTCA	CAGTTGGTCCAAGGTTTGCA
Caspase-3 (M)	CAGCCAACCTCAGAGAGACA	ACAGGCCCATTTGTCCCATA
BAD (M)	TCCTGGGGAGCAACATTCAT	ACCCTCAAACTCATCGCTCA
BCL2 (M)	CTTCAGGGATGGGGTGAACT	ATCAAACAGAGGTCGCATGC
BAX (M)	GAGACACCTGAGCTGACCTT	CCCCAGTTGAAGTTGCCATC
α-SMA (M)	CCCAACTGGGACCACATGG	TACATGCGGGGGACATTGAAG
TGF-β (M)	CTCCCGTGGCTTCTAGTGC	GCCTTAGTTTGGACAGGATCTG
Collagen-I (M)	CCGTGACCTCAAGATGTGCC	GAACCTTCGCTTCCATACTCG
Collagen-III (M)	GACCTCCTGGAAAAGATGGATC	AAATCCATTGGATCATCCCC
β-actin (M)	ATGGAGGGGAATACAGCCC	TTCTTTGCAGCTCCTTCGTT
Nrf2 (H)	GGTTGCCCACATTCCCAAAT	AGCAATGAAGACTGGGCTCT
PGC1α (H)	AGCCTCTTTGCCCAGATCTT	GGCAATCCGTCTTCATCCAC
PPARα (H)	CCCTCCTCGGTGACTTATCC	CACCAGCTTGAGTCGAATCG
SOD2 (H)	CAAAGGGGAGTTGCTGGAAG	AGCAGTGGAATAAGGCCTGT
SOD1 (H)	GGAGACTTGGGCAATGTGAC	CACAAGCCAAACGACTTCCA
NF-κB (H)	AATGGTGGAGTCTGGGAAGG	TCTGACGTTTCCTCTGCACT
NLRP3 (H)	GTTTGACCCCGATGATGAGC	CTTGTGGATGGGTGGGTTTG
TNF-α (H)	CTGAAAGCATGATCCGGGAC	TTAGAGAGAGGTCCCTGGGG
IL-1β (H)	TCCAGCTACGAATCTCCGAC	TGATCGTACAGGTGCATCGT
IL-6 (H)	AGTCCTGATCCAGTTCCTGC	CTACATTTGCCGAAGAGCCC
BAD (H)	GAGGACGACGAAGGGATGG	AAGTTCCGATCCCACCAGG
BCL2 (H)	GCCTTCTTTGAGTTCGGTGG	GAAATCAAACAGAGGCCGCA
BAX (H)	AAGAAGCTGAGCGAGTGTCT	GTTCTGATCAGTTCCGGCAC
β-actin (H)	CTCCATCCTGGCCTCGCTGT	GCTGTCACCTTCACCGTTCC

2.8. Immunofluorescence cytochemistry

After cell fixation, cells were permeabilized with 0.5 % Triton X-100. After rinsing, cells were closed and incubated with anti-NF-κB and PPARα antibodies overnight. After washing, cells were incubated with secondary antibodies followed by counterstaining with DAPI.

2.9. Western blotting

Western blotting was performed as described. Briefly, samples were lysed with lysis buffer. Equal amounts of total protein (40–60 μg) were isolated from each sample and then transferred to a nitrocellulose membrane and incubated with the indicated antibodies. After incubation with secondary antibodies, protein bands are displayed using a chemiluminescence imaging system. All samples in the same group are processed simultaneously.

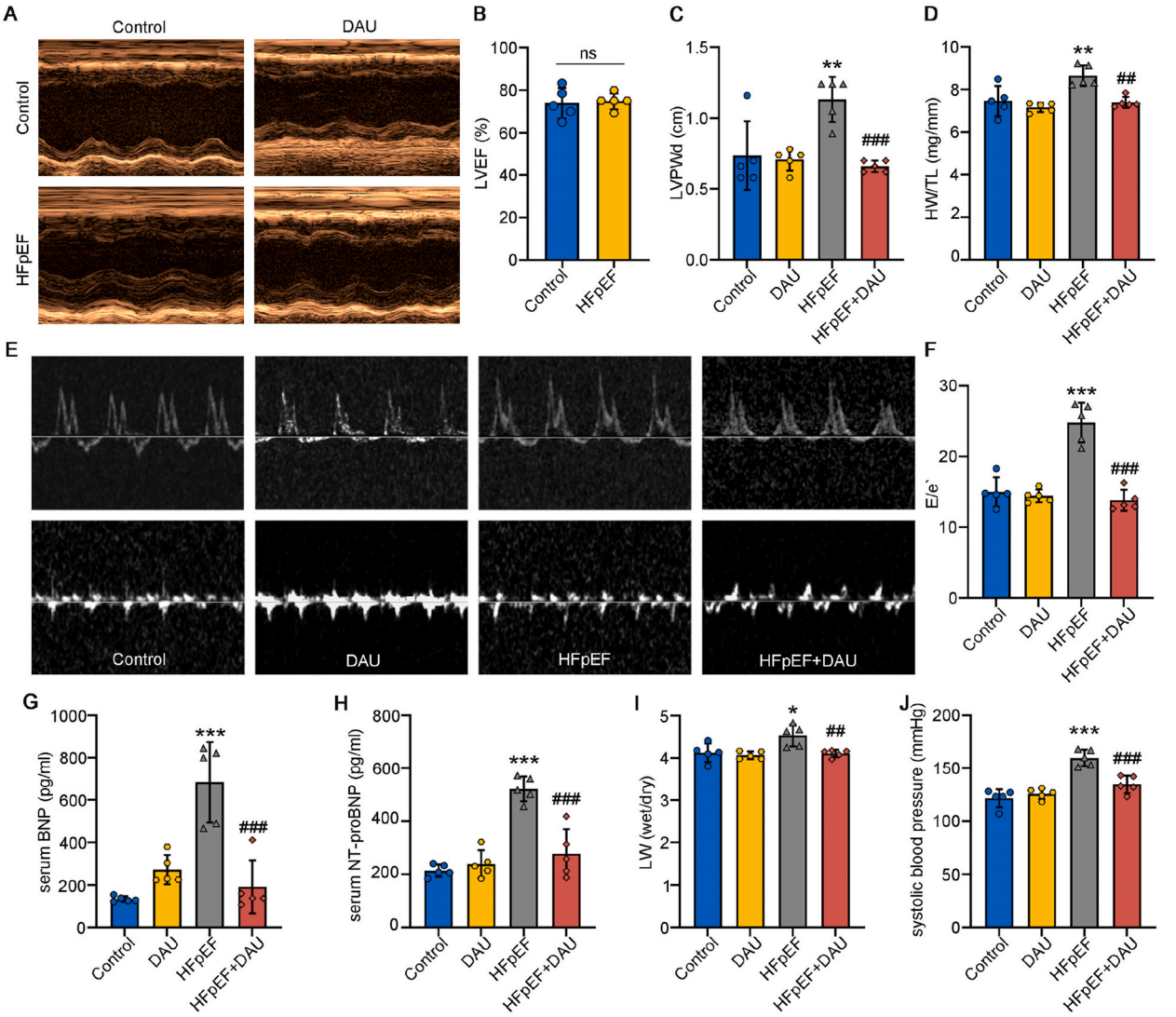

Fig. 1. Daucosterol treatment significantly improves diastolic function in HFpEF mice.
(A) Representative M-mode echocardiographic traces of the left ventricle. (B) Left ventricular ejection fraction. (C) Left ventricular posterior wall degree. (D) Heart weight/tibial length. (E) Typical pulsed wave Doppler (top) and tissue Doppler (bottom). Images are representative of 5 independent mice. (F) Ratio of mitral E peak to e' peak (E/e'). (G–H) Serum BNP, NT-proBNP, was measured by enzyme-linked immunosorbent assay. (I) Ratio of lung wet weight to dry weight (LW). (J) Cardiac systolic blood pressure. Data are mean ± SD using One-Way ANOVA. ns: no statistically significant difference compared to control; $^{*}P < 0.05$, $^{**}P < 0.005$, $^{***}P < 0.0001$ *vs* Control; $^{\#\#}P < 0.005$, $^{\#\#\#}P < 0.0001$ *vs* HFpEF (n ≥ 5).

2.10. Quantitative Real-time PCR (RT-qPCR)

Total RNA was extracted from mouse heart by Trizol, and its purity and concentration were measured by ultramicro spectrophotometer, and reverse transcribed into cDNA. After 3-fold dilution of cDNA, the reaction system was established: 20 μL containing 2 μL cDNA, 10 μL 2 × AceQ qPCR SYBR Green Master Mix, 0.5 μL upstream and downstream primers, and 7 μL sterile water. The PCR procedure was 94 °C 180s, 94 °C 15s, 56 °C 10s, 45 cycles. Three replicates were set for each sample, and β-actin was used as the internal reference to calculate the relative expression of gene mRNA.

The PCR primers were synthesized by GENEWIZ, Inc., the total RNA kit (Trizol) was purchased from Beijing Zhuang meng International Biogene Technology Co and primer sequences are shown in Table 1.

2.11. Statistical analysis

All data involved in this experiment were expressed in the form of means ± standard deviation (SD), and GraphPad Prism software was used for plotting and statistical analysis, and the data were analyzed by One-Way ANOVA and Two-Way ANOVA, with $P < 0.05$ defined as a significant difference.

3. Results

3.1. Daucosterol alleviates heart failure with preserved ejection fraction in mice

Following the previously described protocol, we divided the WT mice into four groups for treatment: normal control (Control), dosed control (DAU), HFpEF model group (HFpEF), and HFpEF model + Daucosterol group (HFpEF + DAU). First, we examined whether DAU administration resulted in modifications to the HFpEF phenotype. The findings indicated that there was no statistically significant variation in LVEF between the Ctrl group and the HFpEF group receiving DAU treatment. Consequently, we concluded that

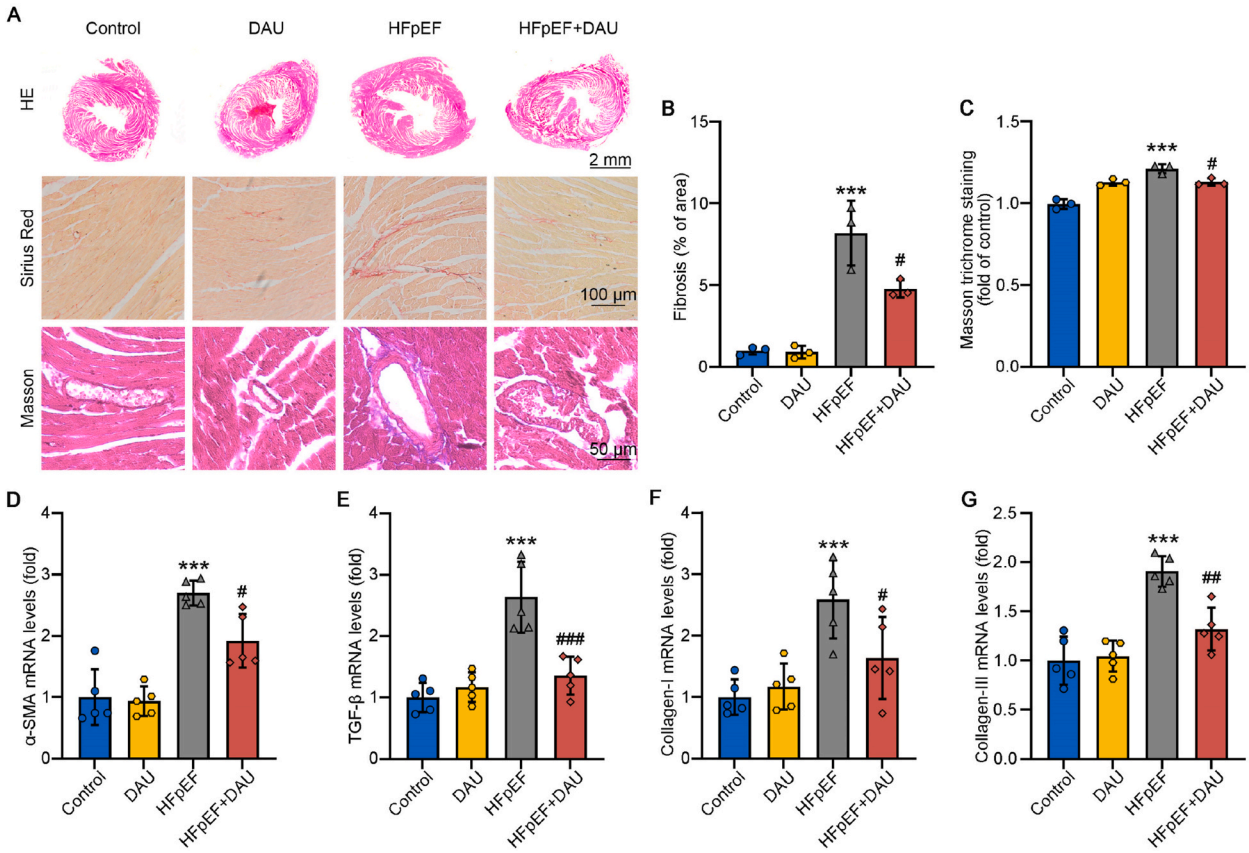

Fig. 2. Daucosterol treatment attenuates myocardial fibrosis in HFpEF mice.
(A) HE staining, Sirius red staining and Masson staining of mouse heart. (B) Percentage of fibrotic area. (C) Masson's trichrome staining. (D–G) Expression of α-SMA, TGF-β, collagen-I, and collagen-III in mouse heart. Data are mean ± SD using One-Way ANOVA. $^{***}P < 0.0001$ *vs* Control; $^{\#}P < 0.05$, $^{\#\#}P < 0.005$, $^{\#\#\#}P < 0.0001$ *vs* HFpEF (n ≥ 5).

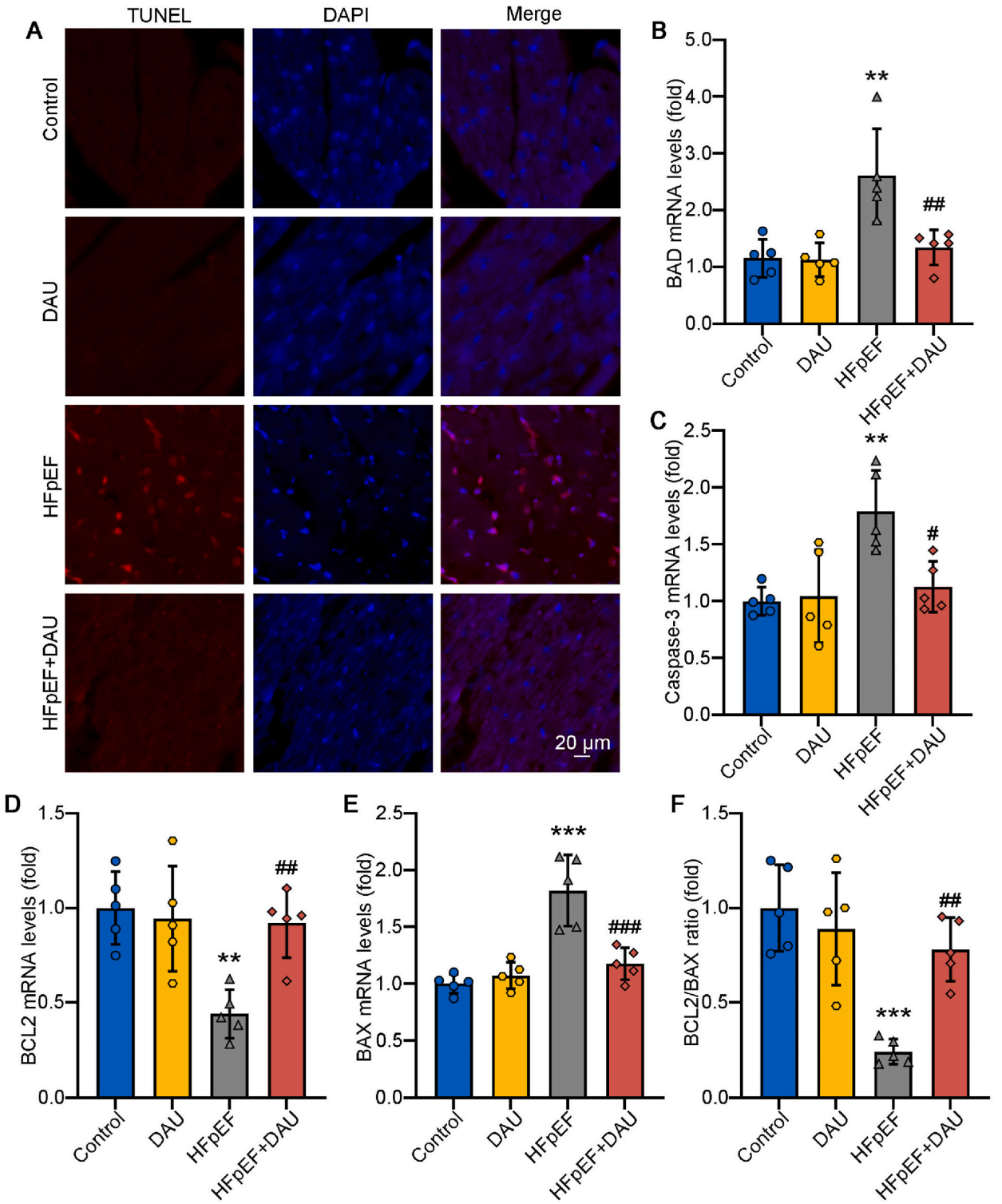

Fig. 3. Daucosterol can improve HFpEF by inhibiting apoptosis.
(A) TUNEL staining of mouse heart, DAPI showing cells number and location. Scale bar: 20 μm. (B–E) Expression of BAD, Caspase-3, BCL2, and BAX in mouse heart. (F) Real-time qPCR was used to calculate BCL2/BAX values in different groups and to compare the anti-apoptotic ability. Data are mean ± SD using One-Way ANOVA. $^{**}P < 0.005$, $^{***}P < 0.0001$ *vs* Control; $^{\#}P < 0.05$, $^{\#\#}P < 0.005$, $^{\#\#\#}P < 0.0001$ *vs* HFpEF (n ≥ 5).

DAU had no effect on the mouse heart's contractile function, suggesting that the two-strike model had no effect on the heart's contractile function (Fig. 1A–B). As shown in Fig. 1C, in the HFpEF model, the left ventricular posterior wall thickness of the heart increased significantly but decreased after DAU treatment. The HFpEF-induced elevated E/e' ratio showed signs of increased left ventricular filling pressure compared with control group (Fig. 1E–F). Preserved ejection fraction and diastolic dysfunction are two important features of HFpEF [16]. Lung congestion is another hallmark feature of HFpEF [17] and DAU significantly attenuated HFpEF-induced lung congestion as shown in Fig. 1D and I. Furthermore, when compared to the Molding set, DAU also reduced heart

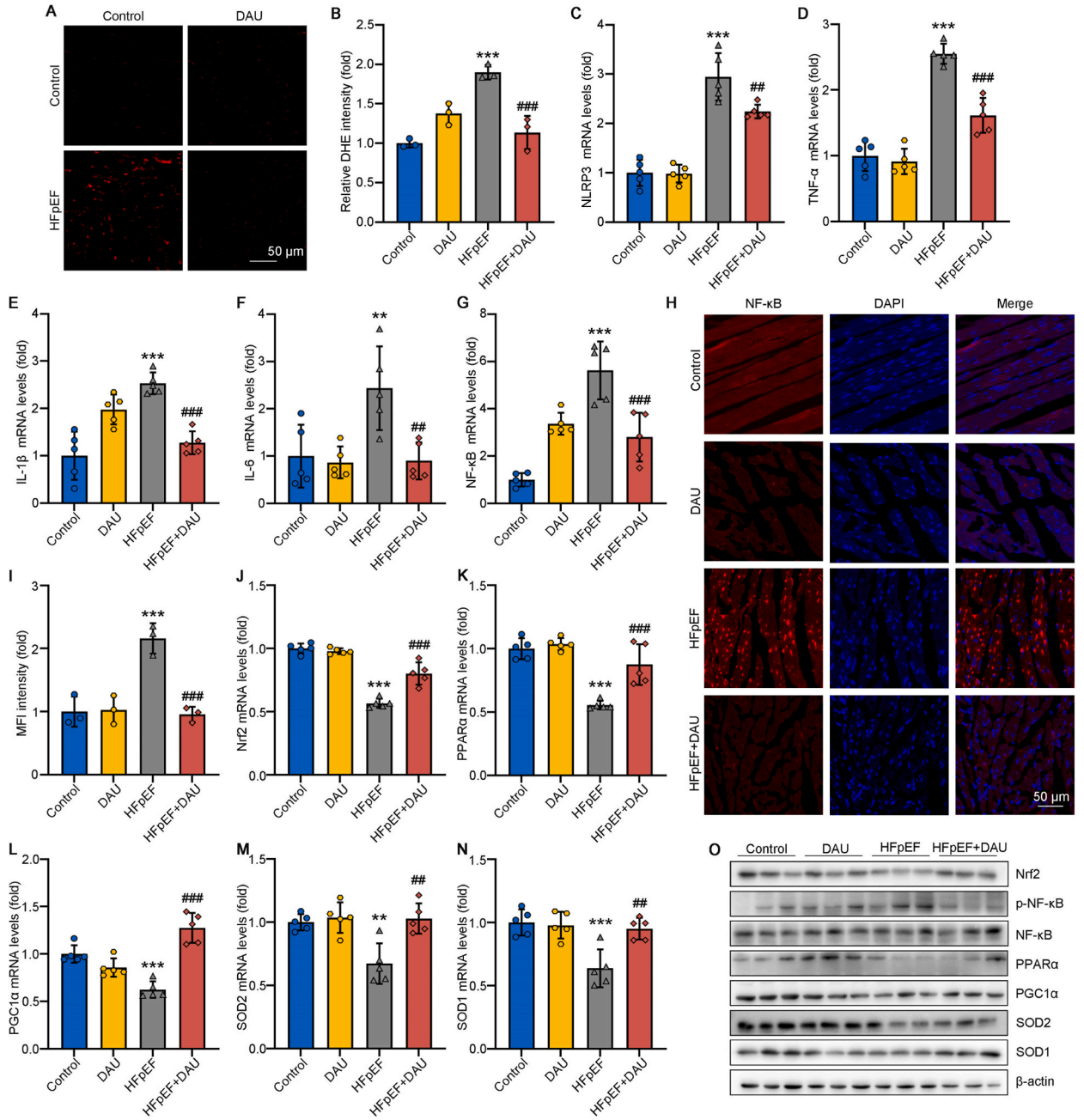

Fig. 4. Daucosterol attenuates cardiac inflammation and activates PPARα in HFpEF mice.
(A) Hepatic DHE staining of mice. scale bar: 50 μm. (B) Statistical analysis of dihydroethidium. (C–G) Expression of NLRP3, TNF-α, IL-1β, IL-6, and NF-κB in mouse heart. (H) Immunofluorescence staining of mouse heart tissue. Scale bar: 50 μm. (I) Statistical analysis of fluorescence. (J–N) Expression of NF-κB, PPARα, PGC1α, SOD1 and SOD2 in mouse heart. (O) Protein expression of Nrf2, p-NF-κB, NF-κB, PPARα, PGC1α, SOD1 and SOD2 in mouse heart. Data are mean ± SD using One-Way ANOVA. $^{**}P < 0.005$, $^{***}P < 0.0001$ *vs* Control; $^{\#\#}P < 0.005$, $^{\#\#\#}P < 0.0001$ *vs* HFpEF (n ≥ 5).

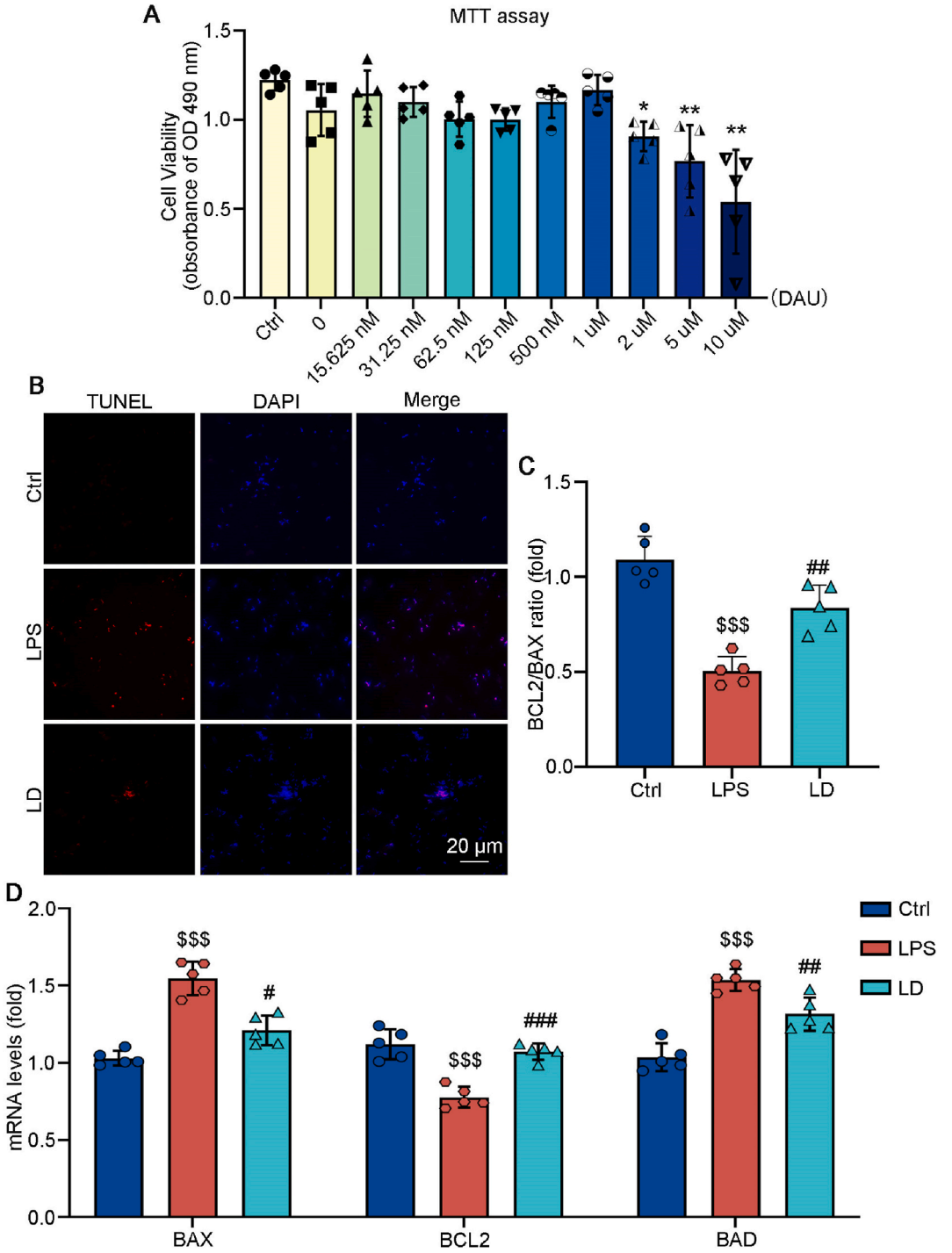

Fig. 5. Daucosterol ameliorates LPS-induced apoptosis of AC16 cells.
(A) AC16 cells viability detection (OD 550 nm absorbance, n ≥ 5). $^{*}P < 0.05$, $^{**}P < 0.01$, $^{***}P < 0.001$ *vs* Normal control group. (B) TUNEL staining of AC16 cells. Scale bar: 20 μm. (C) The BCL2/BAX values of different groups were calculated by RT-qPCR to compare the anti-apoptosis ability. (D) Expression of BAX, BCL2, BAD mRNA in AC16.Data are mean ± SD using Two-Way ANOVA, $^{\$\$\$}P < 0{,}0001$ *vs* Ctrl; $^{\#}P < 0.05$, $^{\#\#}P < 0.005$, $^{\#\#\#}P < 0.005$ *vs* LPS (n ≥ 5).

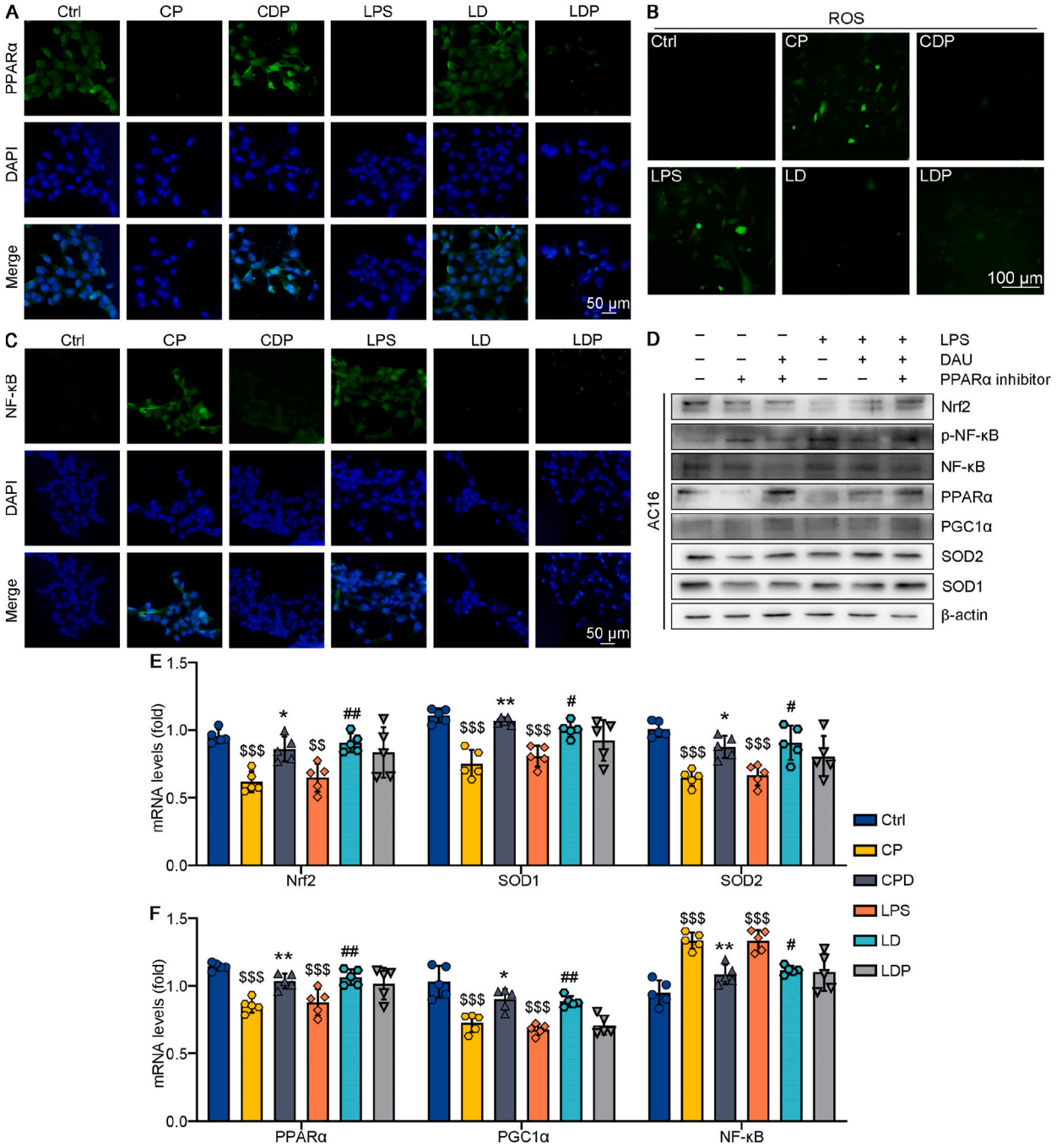

Fig. 6. The effect of DAU on oxidative stress induced by GW6471 and LPS in AC16 cells.
(A) Immunofluorescence staining of PPARα. Scale bar: 50 μm. (B) DCFH-DA staining of AC16 cells. Scale bar:100 μm. (C) Immunofluorescence staining of NF-κB. Scale bar: 50 μm. (D) Protein expression of Nrf2, p-NF-κB, NF-κB, PPARα, PGC1α, SOD1 and SOD2 in AC16 cells. (E–F) Expression of Nrf2, p-NF-κB, NF-κB, PPARα, PGC1α, SOD1 and SOD2 mRNA in AC16 cells. Data are mean ± SD using Two-Way ANOVA, $^{\$\$}P < 0.005$, $^{\$\$\$}P < 0.0001$ *vs* Ctrl; $^{*}P < 0.05$, $^{**}P < 0.005$ *vs* CP; $^{\#}P < 0.05$, $^{\#\#}P < 0.005$ *vs* LPS ($n \geq 5$).

hypertrophy in HFpEF animals. Similarly, following DAU treatment, HFpEF animals showed lower blood pressure, serum BNP, and NT-proBNP levels (Fig. 1G, H and 1J). The above results suggest that DAU significantly improved the cardiac function in HFpEF mice.

3.2. Daucosterol reduces HFpEF-induced myocardial fibrosis

Cardiac fibrosis can cause cardiac stiffness, which has been reported to play an important role in HFpEF [18]. Staining showed that the myocardium in the HFpEF group was significantly hypertrophy and myocardial fibrosis was aggravated, while the cross-sectional area of left ventricular cardiomyocytes in the dau group was significantly smaller than that in the HFpEF group (Fig. 2A–C). Next, we measured the mRNA levels of TGF-β and α-SMA, two genes linked to fibrosis, and discovered that the HFpEF group had considerably higher levels of both genes (Fig. 2D and E). In addition, HFpEF significantly increased the expression of type collagen (Fig. 2F–G). These results suggest that DAU could mitigate myocardial fibrosis and adverse cardiac remodeling in HFpEF mice.

3.3. Daucosterol ameliorates HFpEF-induced apoptosis

To further investigate the therapeutic effect of DAU in HFpEF, we investigated whether DAU could ameliorate the apoptosis caused by HFpEF. First, mouse heart slices were stained with TUNEL. The result showed that the number of apoptotic cells significantly increased in the HFpEF group, but it was reversed after DAU treatment (Fig. 3A). In addition, DAU could promote the transcript levels of anti-apoptotic gene BCL2 and decrease the mRNA expression of the pro-apoptotic genes Caspase-3, BAD, and BAX (Fig. 3B–E). BAX and BCL2 jointly regulate the apoptotic pathway, thus apoptosis can be judged based on the ratio of BCL2/BAX [19]. As shown in Fig. 3F, the heart BCL2/BAX ratio of hfpef mice was recovered after DAU treatment, indicating that DAU enhanced the anti-apoptotic ability of mice and weakened the apoptotic reaction of heart tissue, thus improving the HFpEF in mice.

3.4. Daucosterol attenuates inflammatory response and oxidative stress in HFpEF mice

Early heart failure is typically accompanied by widespread inflammation. Systemic chronic inflammation can then create a vicious loop with oxidative stress, which is a major factor in the pathophysiology of heart failure [20]. To assess the level of myocardial oxidative stress, we performed dihydroethidium staining on fresh heart sections from mice. As shown in Fig. 4A, when compared to the control group, the HFpEF group's mice's heart tissue had higher dihydroethidium fluorescence intensity, however, DAU treatment decreased the fluorescence intensity. Inflammation is a major cause of HFpEF-induced cardiac injury, and the mRNA levels of

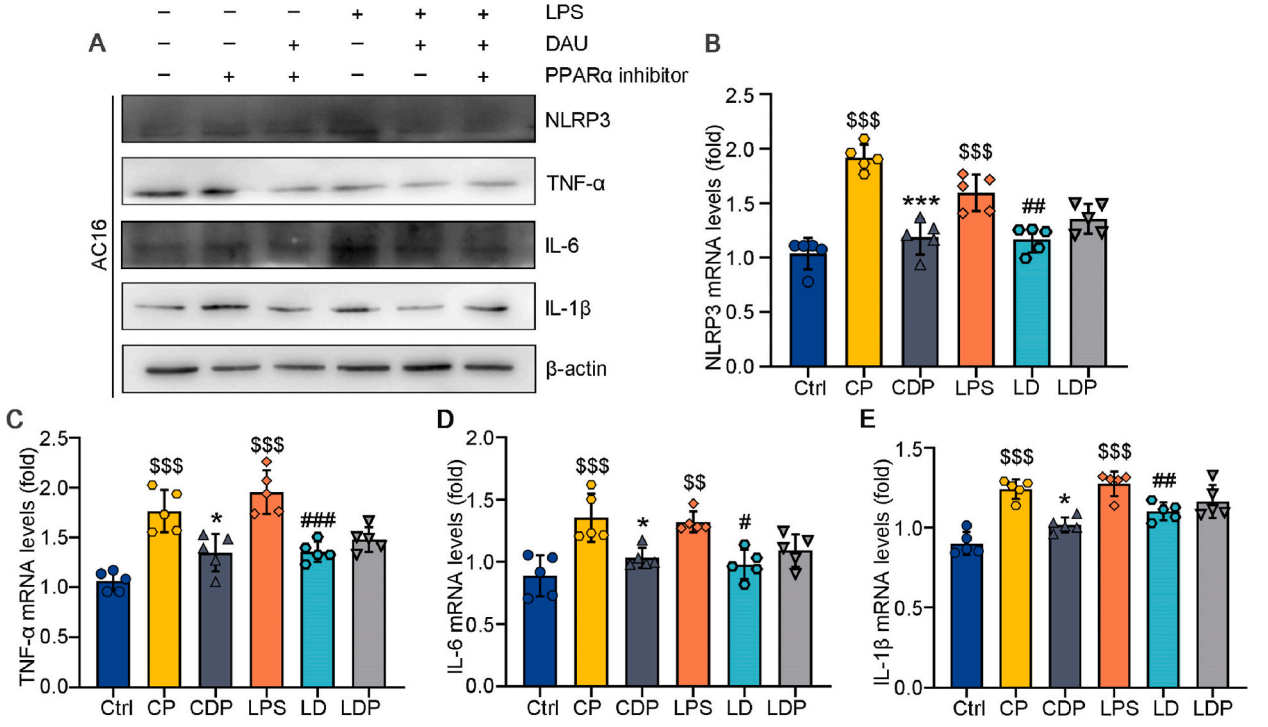

Fig. 7. The effect of DAU on GW6471 and LPS-induced inflammatory factors in human cardiomyocytes.
(A) Protein expression of NLRP3, TNF-α, IL-1β and IL-6 in AC16. (B–E) Expression of NLRP3, TNF-α, IL-1β and IL-6 mRNA in AC16.Data are mean ± SD using Two-Way ANOVA, $^{\$\$}P < 0.005$, $^{\$\$\$}P < 0{,}0001$ *vs* Ctrl; $^{*}P < 0.05$, $^{***}P < 0{,}0001$ *vs* CP; $^{\#}P < 0.05$, $^{\#\#}P < 0.005$, $^{\#\#\#}P < 0.005$ *vs* LPS (n ≥ 5).

inflammation-related genes NLRP3, TNF-α, IL-6, and IL-1β were significantly increased in HFpEF mice, which was decreased by DAU treatment (Fig. 4C–F). As shown in Fig. 4G and I, HFpEF upregulated the degree of phosphorylation of NF-κB in mice and suppressed the expression of Nrf2, PPARα, PGC1α, SOD2, and SOD1 in both mRNA and protein forms (Fig. 4J–O). However, these changes were observably reversed by the treatment of DAU. The above results suggest that DAU significantly ameliorated cardiac inflammation and oxidative stress in HFpEF mice.

3.5. Daucosterol ameliorates LPS-induced apoptosis of AC16 cells

At present, there is no clear cell model of HFpEF. Therefore, we used LPS to induce inflammatory damage in human myocardial AC16 cells, and verified the mechanism of DAU on HFpEF *in vitro*. The optimal concentration of DAU on AC16 cells was first determined by MTT analysis (Fig. 5A). The results showed that the concentration of DAU at 490 nm to produce significant toxic effects on cells was 2 μM. Therefore, we decided to use 1 μM of DAU for subsequent experiments in AC16 cells. According to the results of TUNEL staining, the LPS group had considerably more apoptotic cells than the Ctrl group, however the DAU therapy decreased this number. Next, the transcription of apoptosis-related proteins in cells was detected. It was found that DAU treatment significantly reduced the expression of pro-apoptotic factors BAD and BAX and increased the expression level of anti-apoptotic factor BCL2 (Fig. 5C–D). In summary, DAU can improve the anti-apoptotic ability of AC16 cells and improve LPS-induced apoptosis of AC16 cells.

3.6. DAU alleviates LPS-induced oxidative stress by regulating the PPARα/NF-κB signaling pathway

Based on our results *in vivo*, we found that DAU has significant activity, and has functions such as improving inflammatory response and reducing oxidative stress. To further explore the molecular mechanism of DAU in the treatment of HFpEF. we referred to the existing research results. One of the studies pointed out that PPARα was highly expressed in heart tissue. This suggests that DAU may exert its biological activity by affecting the expression of PPARα. Therefore, we speculate that DAU may regulate the PPARα/NF-κB signaling pathway by restoring the expression of PPARα, thereby reducing the cell inflammatory response and improving the function of HFpEF. To verify this hypothesis, we designed a set of experiments, in which GW6471, an inhibitor of PPARα, was added and co-cultured with DAU. Fig. 6A demonstrated how DAU reversed the trend of downregulating PPARα expression in the LPS and CP groups relative to the Ctrl group. Through ROS staining, we observed that GW6471 significantly increased the level of reactive oxygen species in AC16 cells, which further confirmed the intensification of oxidative stress. At the same time, DAU reduced ROS levels caused by GW6471 and LPS (Fig. 6B). However, when we added DAU to the experimental group, the situation changed. Both at the protein and mRNA levels, we observed a significant decrease in the expression of NF-κB, which means that the inflammatory response has been alleviated. Meanwhile, there was a notable rise in the expression levels of genes linked to energy metabolism and antioxidants, including Nrf2, PGC1α, PPARα, SOD1 and SOD2 (Fig. 6C–F). The results obtained imply that DAU can, in fact, lessen oxidative stress by reestablishing PPARα, which in turn controls the PPARα/NF-κB signaling pathway and shields cells from the outside world.

3.7. Daucosterol alleviates oxidative stress and inflammation by restoring PPARα expression

To explore whether DAU regulates cellular inflammation through PPARα, we investigated the expression of proteins linked to inflammation in AC16 cells and discovered that DAU lowered the expression of inflammatory factors that were upregulated by GW6471 or LPS (Fig. 7A). The results of RT-qPCR also verified the improvement effect of DAU on AC16 cells. DAU not only reduced the mRNA level of NLRP3 in the model group, but also reduced the mRNA levels of NLRP3, TNF-α, IL-6, IL-1β and other inflammatory factors caused by GW6471 (Fig. 7B–E). In summary, DAU has a significant anti-inflammatory effect and can effectively reduce LPS-induced inflammatory response.

4. Discussion

50 % of heart failure patients are caused by HFpEF and compared to heart failure with reduced ejection fraction (HFrEF), HFpEF is more common [21]. HFpEF involves complex interactions between complications such as hypertension, diabetes, renal failure, obesity, and atrial fibrillation and cardiac structural and functional abnormalities such as left ventricular hypertrophy, myocardial fibrosis, myocardial stiffness, endothelial dysfunction, and oxidative stress [22]. These factors raise systemic inflammation, which in turn triggers other diseases such increased deposition of collagen and other matrix proteins, which result in left ventricular hypertrophy and myocardial fibrosis [23–25]. Remodeling of the ventricles and atrium may result from increased fibrosis [26]. In HFpEF, due to myocardial ischemia, hypoxia and other reasons, cardiomyocytes will produce a large amount of ROS, resulting in enhanced oxidative stress response, which will further damage cardiomyocytes and aggravate myocardial dysfunction [27]. In HFpEF, abnormal inflammation and apoptosis can lead to excessive damage and death of cardiomyocytes [28].Inflammation can affect myocardial remodeling and dysfunction through coronary microvascular endothelial dysfunction, thereby inducing reactive interstitial fibrosis and changing the secretory communication between endothelial cells and pericardial cells [29]. Ultimately, the inflammatory response causes cardiomyocytes to produce hypertrophy and stiffness due to a decrease in cyclic guanosine monophosphate (cGMP) and nitric oxide (NO), which impacts left ventricular diastolic dysfunction [30]. Systemic inflammation is thought to be a common biological feature of HFpEF and HFrEF, especially HFpEF[20,31]. In HFpEF, inflammation affects not only the myocardium but also other organs, such as the lungs, skeletal muscle and kidneys. Previous experiments showed that the expression levels of the pro-inflammatory factors TNF-α, IL-6 and IL-1β were significantly increased in HFpEF mice [32]. In *in vivo* experiments, we demonstrated that DAU improves

cardiac diastolic function, such as echocardiographic parameters E/e' ratio, LV posterior wall degree, and reduces serum BNP and NT-proBNP levels and associated with a reduction in LV enlargement and pressure overload; Consistently, pulmonary edema was also significantly improved in the DAU group of mice. When DAU was present, the expression of pro-inflammatory factors (NLRP3, TNF-α, IL-1β, and IL-6) was markedly enhanced in HFpEF mice. In LPS-induced cardiac inflammation model *in vitro*, DAU inhibited the inflammatory response of cardiomyocytes, reduced cellular oxidative stress, and regulated the expression of genes related to inflammation and oxidative stress by recovering PPARα.

Peroxisome proliferator-activated receptors (PPARs) are nuclear receptors that function as ligand-activated transcription factors. They exist in three isoforms: PPARα, PPARβ/δ, and PPARγ [33]. PPARα regulates energy balance, PPARγ activation leads to insulin sensitization and enhances glucose metabolism, and PPARβ/δ activation enhances fatty acid metabolism [34]. Therefore, the nuclear receptor PPAR family plays an important regulatory role in energy homeostasis and metabolic function. The PPAR signaling pathway is present in many different organelles, the most prominent of which is the mitochondria. PPAR is important in the metabolism of fatty acids and has anti-inflammatory and anti-fibrotic properties, as well as regulating the metabolism of glucose and energy [35]. It has been demonstrated that PPARα regulates both acute and chronic inflammation in several different tissues, such as the liver, gut, lung, heart, and vascular wall [36]. Furthermore, PPARα increases cellular fatty acid uptake, esterification, and transport, regulates genes involved in lipoprotein metabolism, and acts as a physiological master switch in the heart, directing cardiac energy metabolism in cardiomyocytes, thereby influencing diabetic cardiomyopathy and pathological heart failure [37]. Although the precise mechanisms underlying both beneficial and worsening effects of PPARα on heart function in animal models remain unknown, numerous metabolic and pathological stress situations have a multifaceted impact on cardiac PPARα expression [38]. As a major nuclear transcription factor protein, NF-κB has been reported to be involved in the cellular inflammatory response [39]. Increasing evidence suggests that ligands of PPARα can negatively regulate the NF-κB pathway and trigger anti-inflammatory responses [40]. Additionally, it has been documented that PPARα activation can prevent NF-κB activation and the production of inflammatory genes that follow [41].

We speculated that DAU could also facilitate PPARα to negatively regulate NF-κB and to improve inflammatory response and regulate oxidative metabolism. To confirm this conjecture, we added PPARα inhibitors in cellular experiments and found that the intracellular PPARα expression levels were significantly reduced after the addition of inhibitors and increased significantly under the co-treatment of inhibitors with DAU.

In this study, we investigated the effect of DAU on HFpEF, and we demonstrated that DAU significantly attenuates myocardial inflammation and oxidative stress and modulates PPARα expression to improve oxidative metabolism, thus, DAU could be a new therapeutic agent for HFpEF.

In summary, DAU attenuates cardiac dysfunction, improves cardiac function and ventricular remodeling in HFpEF mice by recovering PPARα to downregulate NF-κB expression, thereby alleviating the inflammatory response as well as relieving oxidative stress, fibrosis and apoptosis. DAU, as an ideal anti-inflammatory product, has no side effects and is affordable. It can be obtained in daily diet, such as carrot, sweet potato, Dan-Shen root, and other foods, so as to achieve the effect of adjuvant treatment of HFpEF. This work further confirms the prospect of anti-inflammatory therapy in HFpEF and provides new ideas for clinical trials to evaluate the potential value of DAU in HFpEF patients.

Funding

This work was supported by the National Natural Science Foundation of China (NSFC) Grant 82304503 to Shuang Zhang, Anhui Provincial Natural Science Foundation Grant 2308085QH305 to Shuang Zhang, and the Fundamental Research Funds for the Central Universities (Hefei University of Technology) grant JZ2023HGTB0288 to Shuang Zhang.

Data availability

There is no additional data available for this study.

CRediT authorship contribution statement

Jie Zhou: Writing – original draft, Investigation. **Bei Wang:** Writing – original draft, Formal analysis. **Mengyao Wang:** Supervision, Investigation. **Yang Zha:** Formal analysis, Data curation. **Shengyuan Lu:** Validation, Data curation. **Feng Zhang:** Validation. **Ying Peng:** Formal analysis. **Yajun Duan:** Project administration. **Dingrong Zhong:** Project administration. **Shuang Zhang:** Writing – review & editing, Supervision, Resources, Project administration, Funding acquisition.

Declaration of competing interest

The authors declare the following financial interests/personal relationships which may be considered as potential competing interests:Shuang Zhang reports financial support was provided by National Natural Science Foundation of China. Shuang Zhang reports financial support was provided by Anhui Provincial Natural Science Foundation. Shuang Zhang reports financial support was provided by Fundamental Research Funds for the Central Universities (Hefei University of Technology). Yajun DUAN has patent #CN116036107B licensed to The First Affiliated Hospital of USTC (Anhui Provincial Hospital). If there are other authors, they declare that they have no known competing financial interests or personal relationships that could have appeared to influence the work reported in this paper.

Appendix A. Supplementary data

Supplementary data to this article can be found online at https://doi.org/10.1016/j.heliyon.2024.e38379.

References

[1] S.M. Dunlay, V.L. Roger, M.M. Redfield, Epidemiology of heart failure with preserved ejection fraction, Nat. Rev. Cardiol. 14 (10) (2017) 591–602.
[2] R.J. Henning, Diagnosis and treatment of heart failure with preserved left ventricular ejection fraction, World J. Cardiol. 12 (1) (2020) 7–25.
[3] S.J. Shah, D.W. Kitzman, B.A. Borlaug, L. van Heerebeek, M.R. Zile, D.A. Kass, et al., Phenotype-specific treatment of heart failure with preserved ejection fraction: a multiorgan roadmap, Circulation 134 (1) (2016) 73–90.
[4] S. Mishra, D.A. Kass, Publisher Correction: cellular and molecular pathobiology of heart failure with preserved ejection fraction, Nat. Rev. Cardiol. 18 (10) (2021) 735.
[5] Y.C. Chia, L.M. Kieneker, G. van Hassel, S.H. Binnenmars, I.M. Nolte, J.J. van Zanden, et al., Interleukin 6 and development of heart failure with preserved ejection fraction in the general population, J. Am. Heart Assoc. 10 (11) (2021) e018549.
[6] C.J. Rush, C. Berry, K.G. Oldroyd, J.P. Rocchiccioli, M.M. Lindsay, R.M. Touyz, et al., Prevalence of coronary artery disease and coronary microvascular dysfunction in patients with heart failure with preserved ejection fraction, JAMA Cardiol 6 (10) (2021) 1130–1143.
[7] F.A. Wenzl, S. Ambrosini, S.A. Mohammed, S. Kraler, T.F. Luscher, S. Costantino, et al., Inflammation in metabolic cardiomyopathy, Front Cardiovasc Med 8 (2021) 742178.
[8] T. Bui Thanh, Duc L. Vu, H. Nguyen Thanh, V. Nguyen Tien, In vitro antioxidant and anti-inflammatory activities of isolated compounds of ethanol extract from Sanchezia speciosa Leonard's leaves, J Basic Clin Physiol Pharmacol [J] 28 (1) (2017) 79–84.
[9] J. Jang, S.M. Kim, S.M. Yee, E.M. Kim, E.H. Lee, H.R. Choi, et al., Daucosterol suppresses dextran sulfate sodium (DSS)-induced colitis in mice, Int. Immunopharm. 72 (2019) 124–130.
[10] F. Zhang, M. Wang, Y. Zha, J. Zhou, J. Han, S. Zhang, Daucosterol alleviates alcohol-induced hepatic injury and inflammation through P38/NF-kappaB/NLRP3 inflammasome pathway, Nutrients 15 (1) (2023).
[11] G.G. Schiattarella, F. Altamirano, D. Tong, K.M. French, E. Villalobos, S.Y. Kim, et al., Nitrosative stress drives heart failure with preserved ejection fraction, Nature 568 (7752) (2019) 351–356.
[12] M. Hecker, A. Behnk, R.E. Morty, N. Sommer, I. Vadasz, S. Herold, et al., PPAR-alpha activation reduced LPS-induced inflammation in alveolar epithelial cells, Exp. Lung Res. 41 (7) (2015) 393–403.
[13] Y. Chen, Y. Duan, X. Yang, L. Sun, M. Liu, Q. Wang, et al., Inhibition of ERK1/2 and activation of LXR synergistically reduce atherosclerotic lesions in ApoE-deficient mice, Arterioscler. Thromb. Vasc. Biol. 35 (4) (2015) 948–959.
[14] Y. Liang, G. Chen, F. Zhang, X. Yang, Y. Chen, Y. Duan, et al., Procyanidin B2 reduces vascular calcification through inactivation of ERK1/2-RUNX2 pathway, Antioxidants (Basel) [J] 10 (6) (2021).
[15] S. Xu, Y. Wang, M. Yu, D. Wang, Y. Liang, Y. Chen, et al., LongShengZhi capsule inhibits doxorubicin-induced heart failure by anti-oxidative stress, Biomed. Pharmacother. 123 (2020) 109803.
[16] M.A. Pfeffer, A.M. Shah, B.A. Borlaug, Heart failure with preserved ejection fraction in perspective, Circ. Res. 124 (11) (2019) 1598–1617.
[17] C. Withaar, L.M.G. Meems, G. Markousis-Mavrogenis, C.J. Boogerd, H.H.W. Sillje, E.M. Schouten, et al., The effects of liraglutide and dapagliflozin on cardiac function and structure in a multi-hit mouse model of heart failure with preserved ejection fraction, Cardiovasc. Res. 117 (9) (2021) 2108–2124.
[18] M. Shabani, A. Sadeghi, H. Hosseini, M. Teimouri, R. Babaei Khorzoughi, P. Pasalar, et al., Resveratrol alleviates obesity-induced skeletal muscle inflammation via decreasing M1 macrophage polarization and increasing the regulatory T cell population, Sci. Rep. 10 (1) (2020) 3791.
[19] K.C. Akcali, A. Dalgic, A. Ucar, K.B. Haj, D. Guvenc, Expression of bcl-2 gene family during resection induced liver regeneration: comparison between hepatectomized and sham groups, World J. Gastroenterol. 10 (2) (2004) 279–283.
[20] S.P. Murphy, R. Kakkar, C.P. McCarthy, J.L. Januzzi Jr., Inflammation in heart failure: JACC state-of-the-art review, J. Am. Coll. Cardiol. 75 (11) (2020) 1324–1340.
[21] P.A. Heidenreich, B. Bozkurt, D. Aguilar, L.A. Allen, J.J. Byun, M.M. Colvin, et al., 2022 AHA/ACC/HFSA guideline for the management of heart failure: a report of the American college of cardiology/American heart association joint committee on clinical practice guidelines, Circulation 145 (18) (2022) e895–e1032.
[22] V. van Empel, H.P. Brunner-La Rocca, Inflammation in HFpEF: key or circumstantial? Int. J. Cardiol. 189 (2015) 259–263.
[23] H.M. DuBrock, O.F. AbouEzzeddine, M.M. Redfield, High-sensitivity C-reactive protein in heart failure with preserved ejection fraction, PLoS One 13 (8) (2018) e0201836.
[24] B.N. Putko, H. Yogasundaram, G.Y. Oudit, The harbinger of mortality in heart failure with preserved ejection fraction: do GDF-15 levels reflect tandem, deterministic effects of fibrosis and inflammation? Can. J. Cardiol. 30 (3) (2014) 264–266.
[25] V. Zach, F.L. Bahr, F. Edelmann, Suppression of tumourigenicity 2 in heart failure with preserved ejection fraction, Card. Fail. Rev. 6 (2020) 1–7.
[26] H. Fukuta, T. Goto, K. Wakami, T. Kamiya, N. Ohte, Effects of mineralocorticoid receptor antagonists on left ventricular diastolic function, exercise capacity, and quality of life in heart failure with preserved ejection fraction: a meta-analysis of randomized controlled trials, Heart Ves. 34 (4) (2019) 597–606.
[27] A. Mongirdiene, L. Skrodenis, L. Varoneckaite, G. Mierkyte, J. Gerulis, Reactive oxygen species induced pathways in heart failure pathogenesis and potential therapeutic strategies, Biomedicines 10 (3) (2022).
[28] G.W. Cho, F. Altamirano, J.A. Hill, Chronic heart failure: Ca(2+), catabolism, and catastrophic cell death, Biochim. Biophys. Acta 1862 (4) (2016) 763–777.
[29] C. Franssen, S. Chen, A. Unger, H.I. Korkmaz, G.W. De Keulenaer, C. Tschope, et al., Myocardial microvascular inflammatory endothelial activation in heart failure with preserved ejection fraction, JACC Heart Fail 4 (4) (2016) 312–324.
[30] L. van Heerebeek, N. Hamdani, I. Falcao-Pires, A.F. Leite-Moreira, M.P. Begieneman, J.G. Bronzwaer, et al., Low myocardial protein kinase G activity in heart failure with preserved ejection fraction, Circulation 126 (7) (2012) 830–839.
[31] F.J. Carrillo-Salinas, N. Ngwenyama, M. Anastasiou, K. Kaur, P. Alcaide, Heart inflammation: immune cell roles and roads to the heart, Am. J. Pathol. 189 (8) (2019) 1482–1494.
[32] H.J. Yang, B. Kong, W. Shuai, J.J. Zhang, H. Huang, MD1 deletion exaggerates cardiomyocyte autophagy induced by heart failure with preserved ejection fraction through ROS/MAPK signalling pathway, J. Cell Mol. Med. 24 (16) (2020) 9300–9312.
[33] N. Wagner, K.D. Wagner, The role of PPARs in disease, Cells 9 (11) (2020).
[34] K.D. Wagner, N. Wagner, Peroxisome proliferator-activated receptor beta/delta (PPARbeta/delta) acts as regulator of metabolism linked to multiple cellular functions, Pharmacol. Ther. 125 (3) (2010) 423–435.
[35] S. Francque, G. Szabo, M.F. Abdelmalek, C.D. Byrne, K. Cusi, J.F. Dufour, et al., Nonalcoholic steatohepatitis: the role of peroxisome proliferator-activated receptors, Nat Rev Gastroenterol Hepatol [J] 18 (1) (2021) 24–39.
[36] N.R. Das, B. Vaidya, P. Khare, M. Bishnoi, S.S. Sharma, Combination of peroxisome proliferator-activated receptor gamma (PPARgamma) agonist and PPAR gamma Co-activator 1alpha (PGC-1alpha) activator ameliorates cognitive deficits, oxidative stress, and inflammation in rodent model of Parkinson's disease, Curr Neurovasc Res 18 (5) (2021) 497–507.
[37] D. Montaigne, L. Butruille, B. Staels, PPAR control of metabolism and cardiovascular functions, Nat Rev Cardiol [J] 18 (12) (2021) 809–823.
[38] K. Drosatos, N.M. Pollak, C.J. Pol, P. Ntziachristos, F. Willecke, M.C. Valenti, et al., Cardiac myocyte KLF5 regulates ppara expression and cardiac function, Circ. Res. 118 (2) (2016) 241–253.

[39] A.E. Irvin, G. Jhala, Y. Zhao, T.S. Blackwell, B. Krishnamurthy, H.E. Thomas, et al., NF-kappaB is weakly activated in the NOD mouse model of type 1 diabetes, Sci. Rep. 8 (1) (2018) 4217.
[40] J. Shen, J. Cheng, S. Zhu, J. Zhao, Q. Ye, Y. Xu, et al., Regulating effect of baicalin on IKK/IKB/NF-kB signaling pathway and apoptosis-related proteins in rats with ulcerative colitis, Int. Immunopharm. 73 (2019) 193–200.
[41] K. De Bosscher, W. Vanden Berghe, G. Haegeman, Cross-talk between nuclear receptors and nuclear factor kappaB, Oncogene 25 (51) (2006) 6868–6886.